

MOF-derived nitrogen-doped porous carbon nanofibers with interconnected channels for high-stable Li⁺/Na⁺ battery anodes

Kainian Chu,^{a,b} Mulin Hu,*^a Bo Song,^a Senlin Chen,^a Junyu Li,^a Fangcai Zheng,^b Zhiqiang Li,^b Rui Li,^a and Jingya Zhou^a

^a Hefei Technology College, Hefei 230011, China

^b Institutes of Physical Science and Information Technology and Key Laboratory of Structure and Functional Regulation of Hybrid Materials of Ministry of Education, Anhui University, Hefei, 230601, China

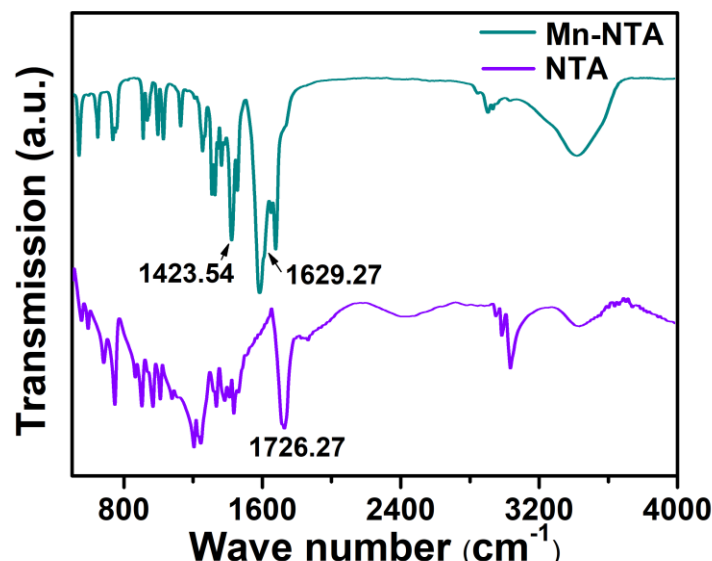


Fig. S1 The Fourier transform infrared spectroscopy (FTIR) spectrum of Mn-NTA and NTA.

* hml@htc.edu.cn

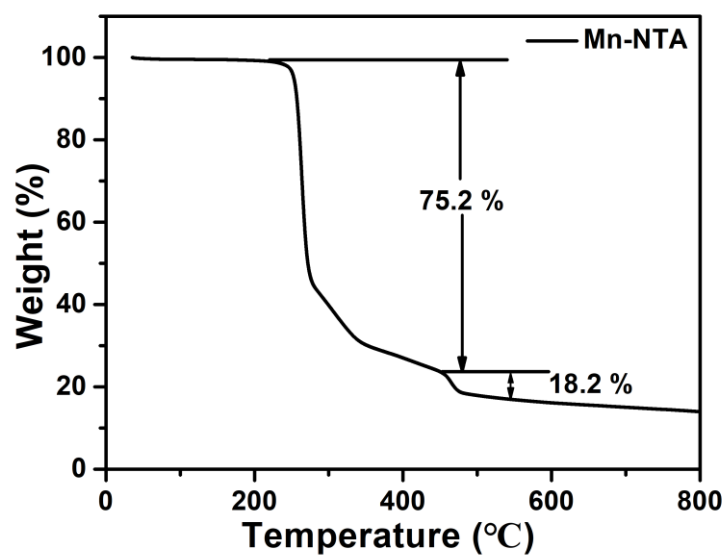


Fig. S2 TGA curve of Mn-NTA nanowires.

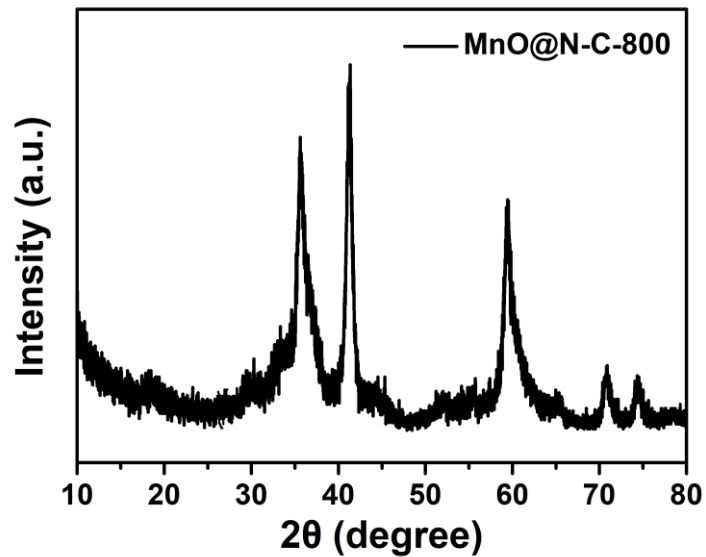


Fig. S3 The XRD pattern of MnO@N-C-800.

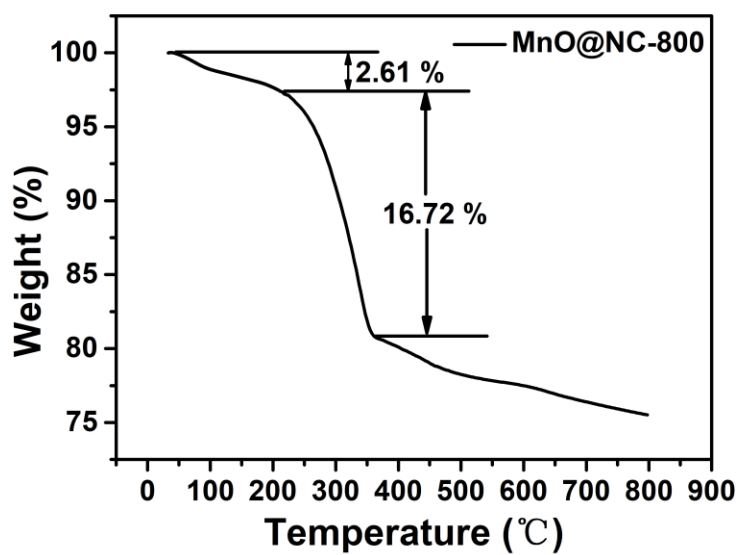


Fig. S4 The TGA curve of MnO@NC-800 in air.

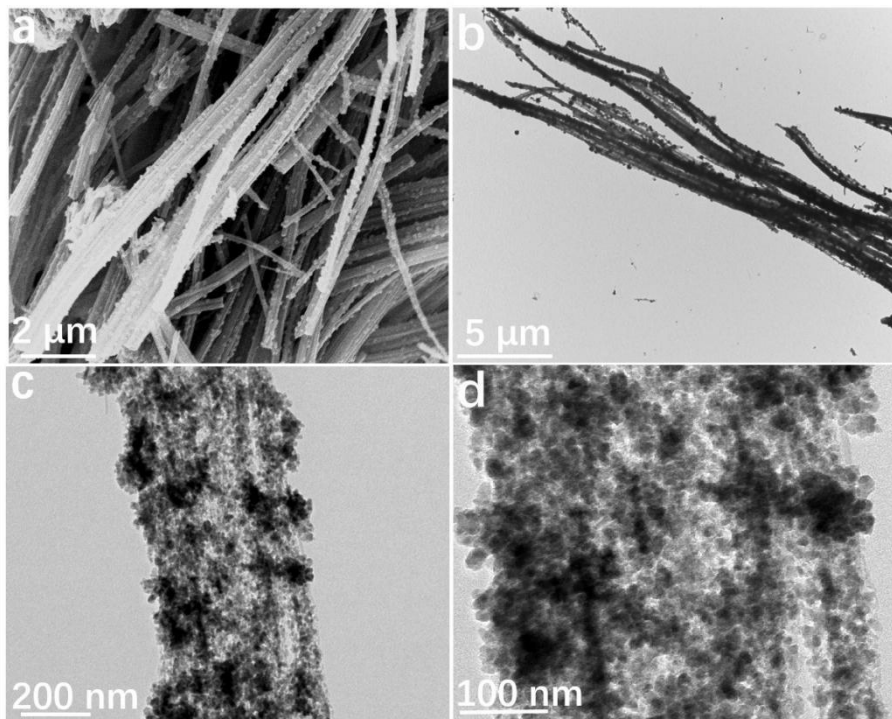


Fig. S5 (a) SEM and (b,c,d) TEM images of MnO@NC-800.

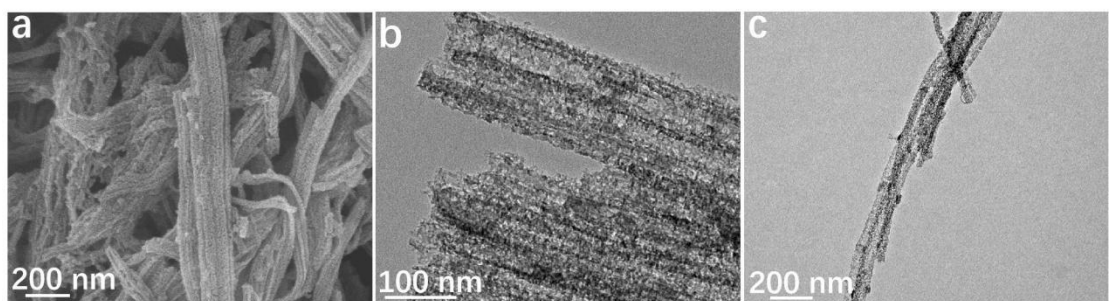


Fig. S6 (a) SEM and (b,c) TEM images of NCNFs-600.

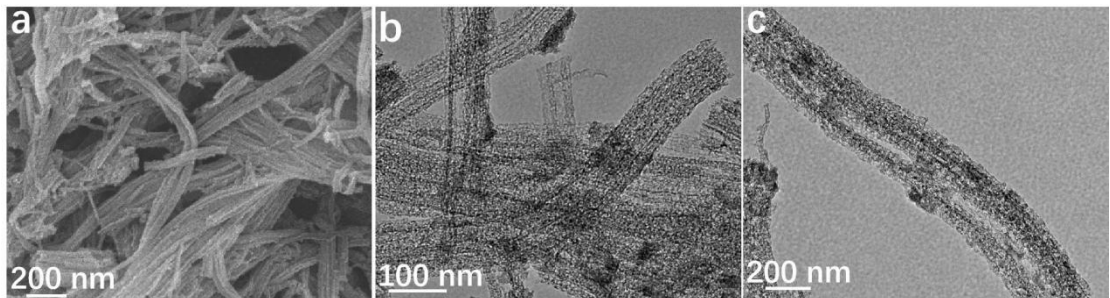


Fig. S7 (a) SEM and (b,c) TEM images of NCNFs-700.

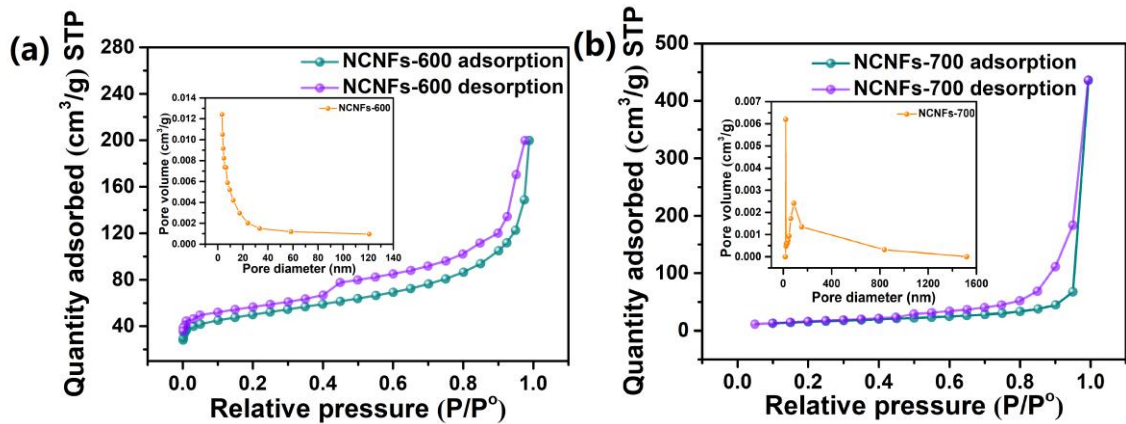


Fig. S8 Nitrogen adsorption-desorption isotherm curves of NCNFs-600 and NCNFs-700.

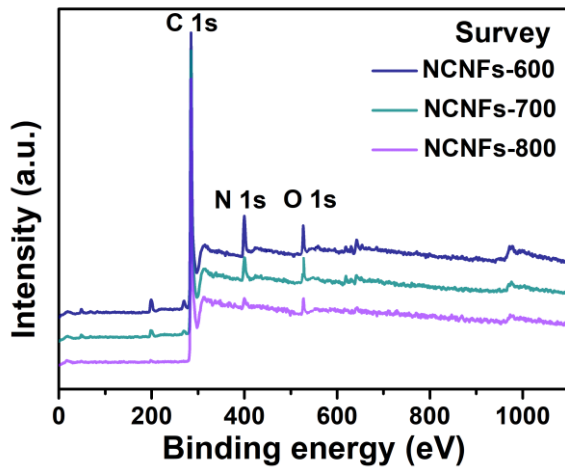


Fig. S9 The full spectra of NCNFs.

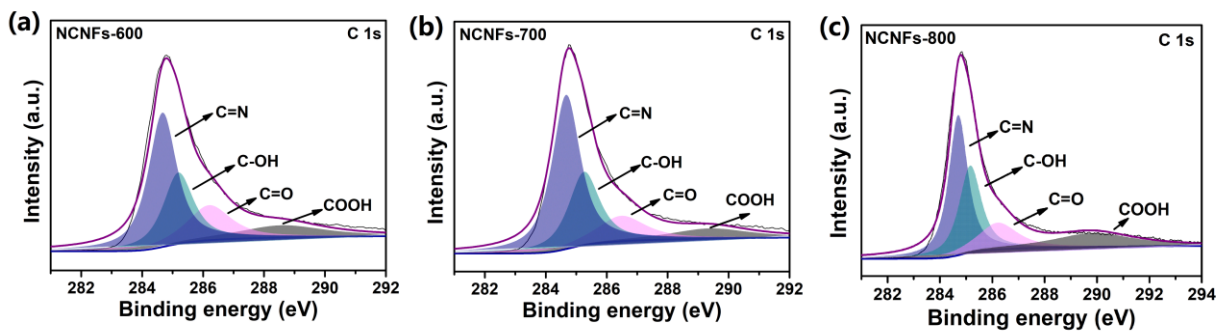


Fig. S10 The C 1s spectra of NCNFs.

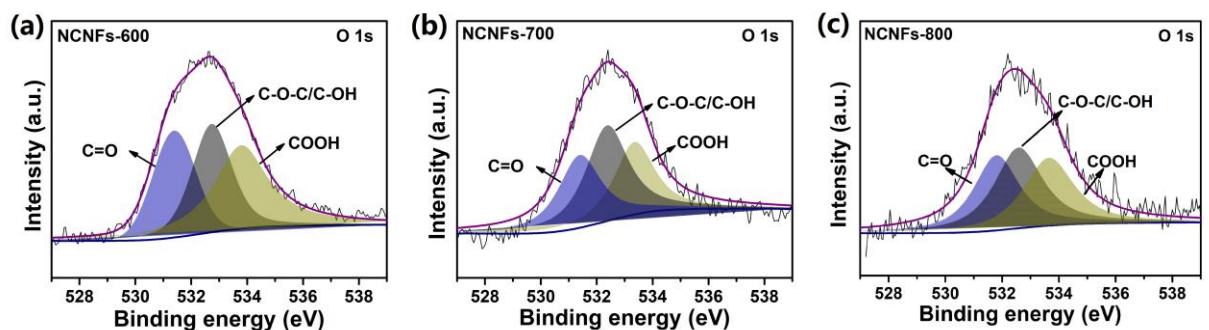


Fig. S11 The O 1s spectra of NCNFs.

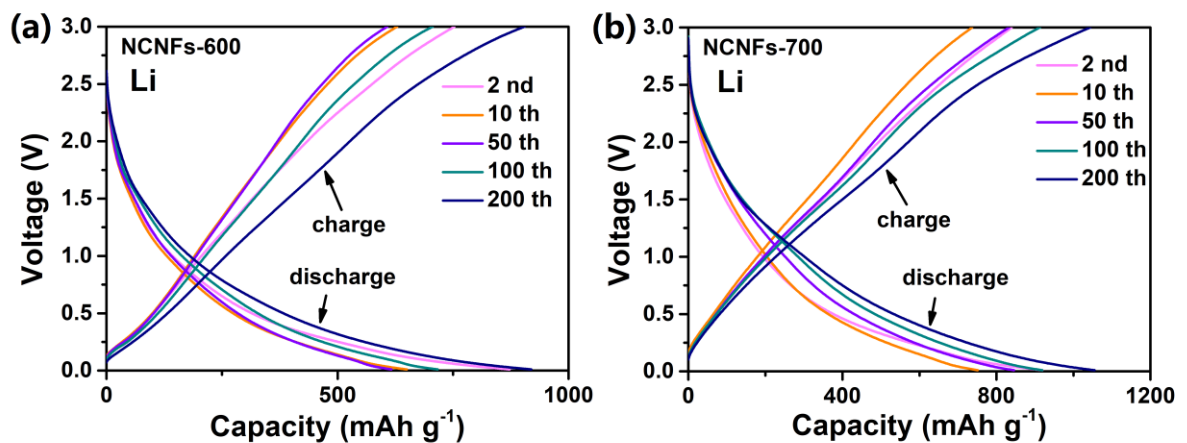


Fig. S12 Discharge/charge profiles of NCNFs-600 and NCNFs-700 at 0.1 A g^{-1} in Li^+ half cells.

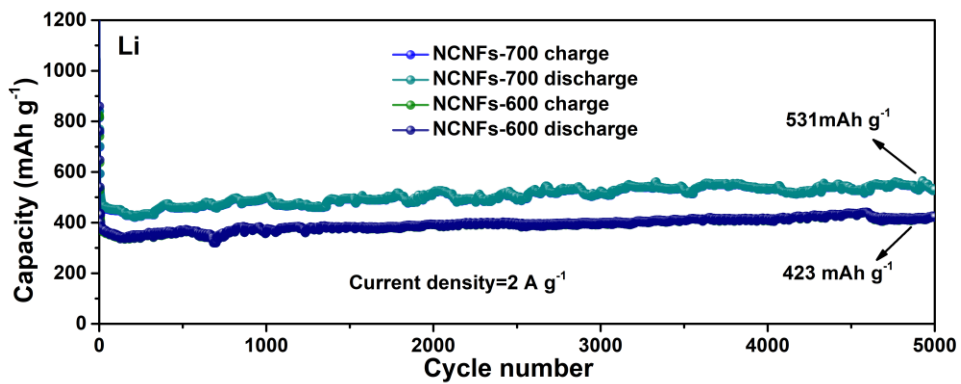


Fig. S13 The cycling performance of NCNFs-600 and NCNFs-700 at 2 A g^{-1} in Li^+ half cells.

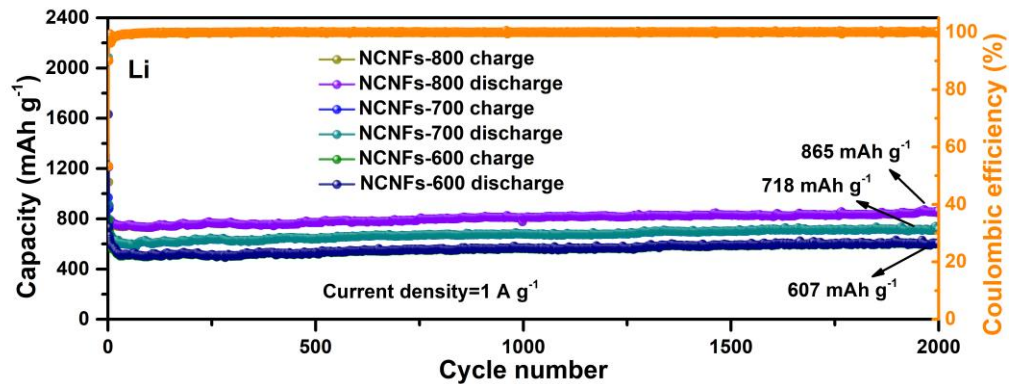


Fig. S14 The cycling performance of NCNFs at 1 A g^{-1} in Li^+ half cells.

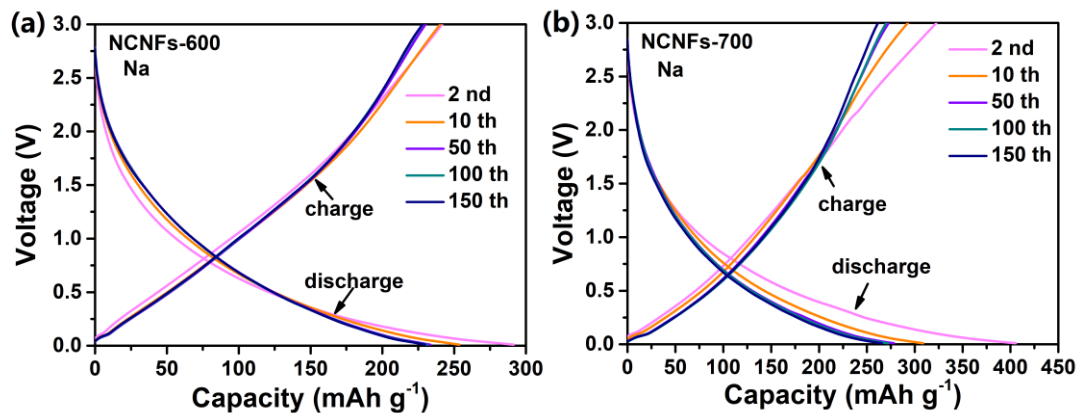


Fig. S15 Discharge/charge profiles of NCNFs-600 and NCNFs-700 at 0.1 A g^{-1} in Na^+ half cells.

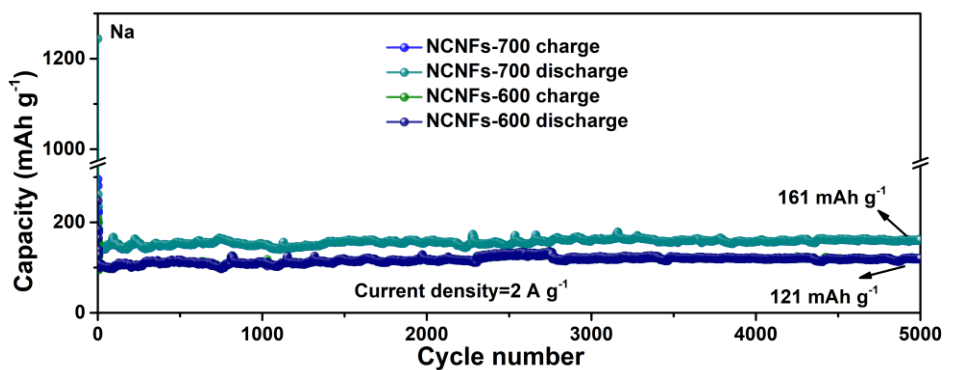


Fig. S16 The cycling performance of NCNFs-600 and NCNFs-700 at 2 A g^{-1} in Na^+ half cells.

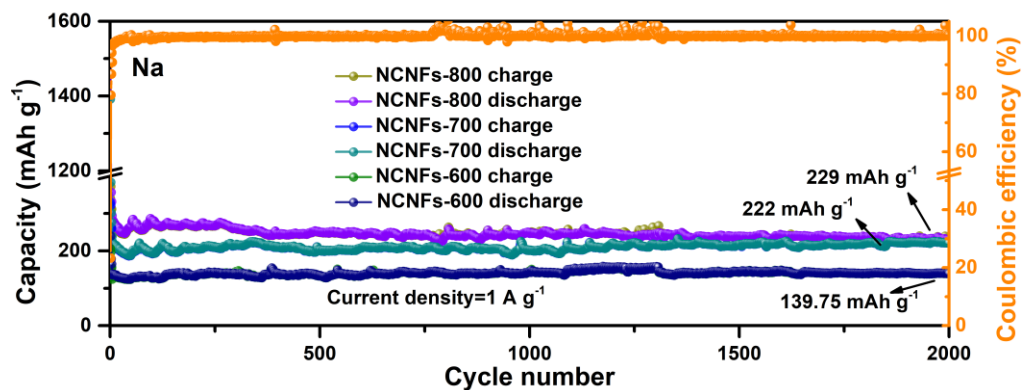


Fig. S17 The cycling performance of NCNFs at 1 A g^{-1} in Na^+ half cells.

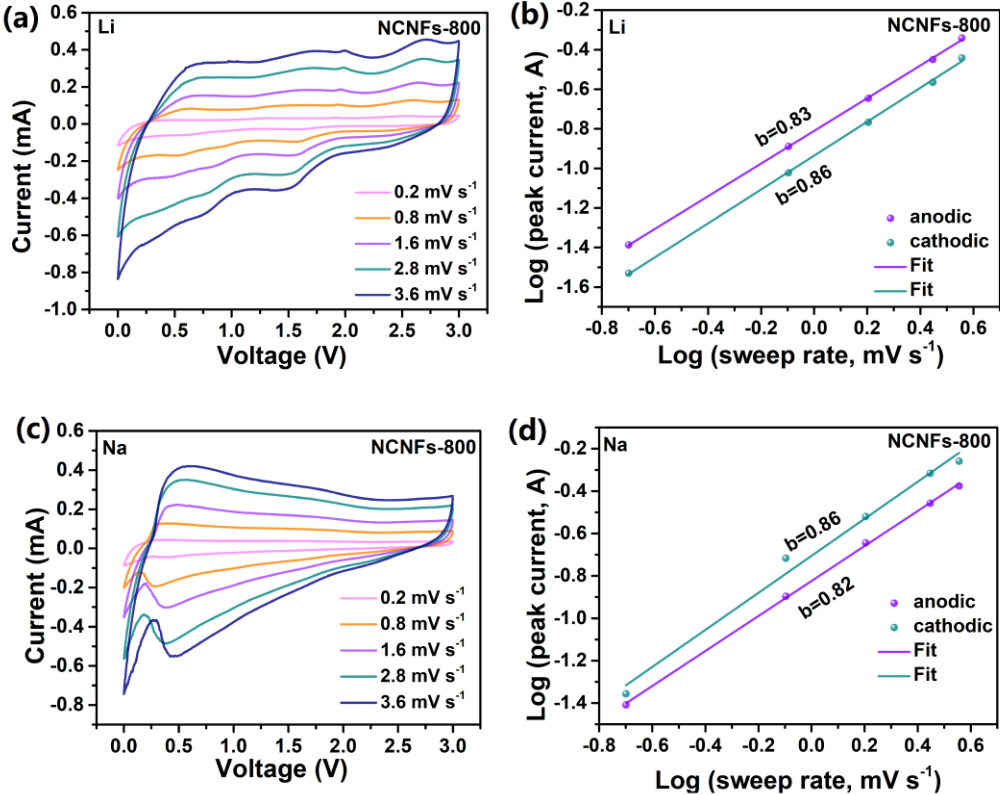


Fig. S18 (a, c) CV curves of NCNFs-800 at different scan rates of 0.2 to 3.6 mV s⁻¹ in Li⁺/Na⁺ half cells. (b, d) The b values of NCNFs-800 in Li⁺/Na⁺ half cells.

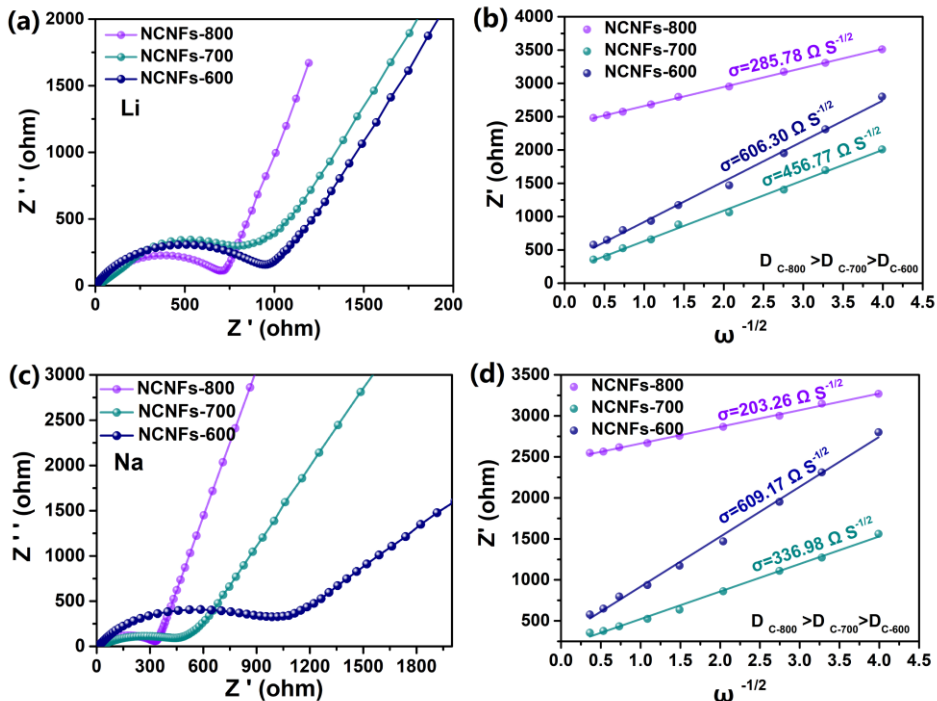


Fig. S19 (a, c) EIS curves of NCNFs in Li⁺/Na⁺ half cells. (b, d) The linear fits of the Z' versus ω^{-1/2} in the low-frequency region of NCNFs in Li⁺/Na⁺ half cells.

Table S1 The corresponding elemental contents of NCNFs.

Sample	Element content (at%)			N-6 (wt%)	N-5 (wt%)	N-Q (wt%)
	C	N	O			
NCNFs-600	81.71	14.05	4.21	28.47	51.80	19.73
NCNFs-700	87.52	9.85	2.63	32.67	44.26	23.07
NCNFs-800	93.27	5.31	1.42	34.09	39.68	26.23

Table S2. Comparison of NCNFs-800 with some related carbon anodes for LIBs at low current densities.

Samples	Current density (mA g ⁻¹)	Cycle number	Capacity (mAh g ⁻¹)	Ref.
NCNFs-800	100	200	1237	Our work
PTA-700	100	100	535	1
WTC-C	300	400	350	2
OSPC-1	200	100	748	3
PVP-HC	400	200	256	4
MES600	500	450	144	5
SGHC-1000	50	100	366	6

Table S3. Comparison of NCNFs-800 with some related carbon anodes for SIBs at low current densities.

Samples	Current density (mA g ⁻¹)	Cycle number	Capacity (mAh g ⁻¹)	Ref.
NCNFs-800	100	150	323	Our work
PLHC-N-1000	25	100	351	7
HC-900	50	200	330	8
3DHPCM-800	100	100	314	9
BC-2H	50	100	334	10
SCNs	100	250	155	11
NOPCP-600	100	100	313	12

References

- 1 G. Huang, Q. Q. Kong, W. T. Yao and Q. Y. Wang, *J. Colloid Interf.*, 2023, **629**, 832-845
- 2 T. Veldevi, S. Raghu, R. Kalaivani and A. Shanmugharaj, *Chemosphere*, 2022, **288**, 132438.
- 3 Z. Q. Zhao, S. Das, G. L. Xing, P. Fayon, P. Heasman, M. Jay, S. Bailey, C. Lambert, H. Yamada, T. Wakihara, A. Trewin, T. Ben, S. L. Qiu and V. Valtchev, *Angew. Chem. Int. edit.*, 2018, **57**, 11952-11956.
- 4 M. J. He, L. Q. Xu, B. Feng, J. B. Hu, S. S. Chang, G. G. Liu, Y. Liu and B. H. Xu, *Molecules*, 2022, **27**, 6994.
- 5 M. X. Song, L. J. Xie, J. Y. Cheng, Z. L. Yi, G. Song, X. Y. Jia, J. P. Chen, Q. G. Guo and C. M. Chen, *J. Energy Chem.*, 2022, **66**, 448-458.
- 6 K. Wang, Y. B. Xu, H. Wu, R. L. Yuan, M. Zong, Y. Li, V. Dravid, W. Ai and J. S. Wu, *Carbon*, 2021, **178**, 443-450.
- 7 W. Nie, H. Cheng, X. Liu, Q. Sun, F. Tian, W. Yao, S. Liang, X. Lu and J. Zhou, *J. Power Sources*, 2022, **522**, 230994.
- 8 J. Wang, Y. S. Li, P. Liu, F. Wang, Q. R. Yao, Y. J. Zou, H. Y. Zhou, M. S. Balogun and J. Q. Deng, *J. Cent. South Univ.*, 2021, **28**, 361-369.
- 9 G. Q. Zou, H. S. Hou, X. Y. Cao, P. Ge, G. G. Zhao, D. L. Yin, X. B. Ji, *J. Mater. Chem. A.*, 2017, **545**, 23550-23558.
- 10 Z. F. Sun, Y. X. Chen, B. J. Xi, C. Geng, W. J. Guo, Q. C. Zhuang, X. G. An, J. Liu, Z. C. Ju and S. L. Xiong, *Energy Storage Mater.*, 2022, **53**, 482-491.
- 11 M. Sun, Y. Qu, F. Zeng, Y. Yang, K. Xu, C. Yuan and Z. H. Lu, *Ind. Eng. Chem. Res.*, 2022, **61**, 2126-2135.
- 12 Z. Q. Li, L. Cai, K. N. Chu, S. K. Xu, G. Yao, L. Z. Wei and F. C. Zheng, *Dalton Trans.*, 2021, **50**, 4335.